ISSN 1062-8738, Bulletin of the Russian Academy of Sciences: Physics, 2008, Vol. 72, No. 11, pp. 1456–1461. © Allerton Press, Inc., 2008.
Original Russian Text © A.V. Gostev, S.A. Ditsman, V.V. Zabrodskii, N.V. Zabrodskaya, F.A. Luk'yanov, E.I. Rau, R.A. Sennov, V.L. Sukhanov, 2008, published in Izvestiya Rossiiskoi Akademii Nauk. Seriya Fizicheskaya, 2008, Vol. 72, No. 11, pp. 1539–1544.

Characterization of Semiconductor Detectors of (1–30)-keV Monoenergetic and Backscattered Electrons

A. V. Gostev[a], S. A. Ditsman[a], V. V. Zabrodskii[b], N. V. Zabrodskaya[b], F. A. Luk'yanov[c], E. I. Rau[a], R. A. Sennov[c], and V. L. Sukhanov[b]

[a] *Institute of Microelectronics Technology and High Purity Materials, Russian Academy of Sciences, Chernogolovka, Moscow oblast, 142432 Russia*
e-mail: Rau@phys.msu.ru

[b] *Ioffe Physicotechnical Institute, Russian Academy of Sciences, Politekhnicheskaya ul. 26, St. Petersburg, 194021 Russia*

[c] *Moscow State University, Moscow, 119992 Russia*

Abstract—Semiconductor detectors of backscattered electrons are basic elements of all modern scanning electron microscopes. Their quality is determined by the properties of planar *p–n* junctions and the parameters of the protective layer on the detector surface. The main characteristics of semiconductor detectors are considered, their response functions are calculated, and the threshold signal cutoff energies are found both for a monoenergetic electron beam and for detection of the total energy spectrum of backscattered electrons. The experimental results are in good agreement with the computational model data.

DOI: 10.3103/S1062873808110026

INTRODUCTION

Semiconductor electron detectors based on silicon shallow-buried *p–n* junctions are widely used in modern electron-probe instruments, for example, in scanning electron microscopes (SEMs). The properties and characteristics of such detectors were investigated, in particular, in [1–4]. A signal I_β of such detectors is determined by the expression [5]

$$I_\beta = I_0 \eta d\Omega \left(1 - \eta_{Si}\frac{\bar{E}_{Si}}{\bar{E}}\right)\frac{\bar{E} - E_{th}}{E_i}C, \quad (1)$$

where I_0 is the electron-probe current; η is the electron backscattering coefficient for a sample; $\bar{E}$ is the average energy of electrons backscattered from the sample; $d\Omega$ is the solid angle of backscattered electron collection for a given detector; η_{Si} is the electron backscattering coefficient for the silicon detector; $\bar{E}_{Si}$ is the average energy of the electrons backscattered from the detector; E_{th} is the detector threshold energy; E_i is the energy of electron–hole pair generation in Si (E_i = 3.65 eV); and C is the charge collection efficiency at the *p–n* junction.

However, the experiments show that relation (1) is valid only at $\bar{E} = E_0$ and E_{th} = const, i.e., for a monoenergetic electron beam with an energy E_0. Actually, backscattered electrons with different energies are incident on a detector, and their flux is determined by the entire energy spectrum of the electrons backscattered from a given sample; therefore, E_{th} is not a constant.

Let us consider in more detail all the components of relation (1) for a detected signal and for the detector response function $\Theta = I_\beta/I_0(E_0/q)$, which characterizes the efficiency of a real detector on the whole. First, we will analyze the above-mentioned characteristics for a monoenergetic electron beam incident on a detector with an energy E_0 and a current I_0 and then generalize the consideration to the entire spectrum of backscattered electrons.

1. CHARACTERISTICS OF A DETECTOR IRRADIATED BY A MONOENERGETIC ELECTRON BEAM

A detected signal can be written (for a monoenergetic electron beam) as

$$I_\beta = I_0(E_0/E_i)(1 - A)(1 - B)CD, \quad (2)$$

where A is the loss of the total beam energy due to the absorption in the passive protective coating of the detector and partially in the low-resistivity top layer of the *p–n* junction, which do not contribute to the charge-carrier generation; B is the loss due to the flux with the total energy $\eta_{Si}\bar{E}_{Si}$, backscattered from the detector; C is the efficiency of charge collection at the *p–n* junction; and D is the detector quality factor, determined by the real current–voltage (I–V) characteristic of the diode. The coefficient C is close to unity in the absence of carrier recombination in the space-charge region with a depth w, provided that the carrier generation region, determined by the total electron range $R_0(E_0)$, is smaller than w. If $R_0(E_0) > w$, it is necessary to take into account

the additional signal decay due to the finite diffusion length L of minority carriers.

The contribution of the factor C to (2) can be estimated from the expression [6]

$$C = \left(\frac{1-\exp(-\gamma)}{\gamma}\right)\exp\left(-\frac{R_0-w}{L}\right), \quad (3)$$

where $\gamma = w/\mu\varepsilon\tau$ (ε is the barrier field of the p–n junction and μ and τ are, respectively, the mobility and lifetime of minority carriers).

Along with the physico-technological factor C, there is another technical reason for the decrease in the signal I_β. The presence of the shunting resistance R_{sh} of the p–n junction in a real detector circuit, the ohmic resistance of imperfect contacts, and the resistance R_S of the high-resistivity base change the I–V characteristic of an ideal diode [7]: $I_\beta = I_S[\exp(qV/kT) - 1] - I_{\beta 0}$, where I_β is the measured current in the external circuit, $I_{\beta 0}$ is the electron-induced current through the p–n junction, I_S is the inverse saturation current through the p–n junction, kT/q is the thermal potential in the semiconductor crystal, and V is the electron-beam-induced potential at the barrier. The presence of spurious resistances in the detector circuit changes the I–V characteristic [7] as follows:

$$\frac{q}{kT}(V - I_\beta R_S) = \ln\left(\frac{I_\beta + I_{\beta 0}}{I_S} - \frac{V - I_\beta R_S}{I_S R_{sh}} + 1\right). \quad (4)$$

The term containing R_{sh} in this expression is generally small; therefore, the current in the external detection circuit can be written as

$$\begin{aligned} I_\beta &= I_S\{\exp[(q/kT)(V - I_\beta R_S)] - 1\} - I_{\beta 0} \\ &\approx I_S(q/kT)(V - I_\beta R_S) - I_{\beta 0}. \end{aligned} \quad (5)$$

Introducing the designation $K = I_S q/kT$, we obtain an approximate estimate for the relationship between I_β and $I_{\beta 0}$ (taking into account that $KV \approx 0$): $I_\beta = I_{\beta 0}/(1 + KR_S) = I_{\beta 0}D$, where $D = 1/(1 + KR_S)$. This dependence indicates that the detected signal I_β is inversely proportional to the resistance R_S in the measurement circuit.

Note that it is difficult to calculate exactly the quality factor of a semiconductor detector as a whole (which is determined by the product CD) because there are many a priori unknown parameters. Therefore, it is more expedient to determine CD experimentally by comparing the calculated and measured values of I_β.

In contrast to all previous calculations of the detector response [1–5], we will consider here separately the electron current and energy losses on reflection and absorption for a dead layer of the protective oxide coating with a thickness d on the detector surface and in the Si crystal. It is only the total energy $I_A(\mathrm{Si})\bar{E}_A(\mathrm{Si})$ absorbed in the semiconductor material that makes a contribution to the I_β signal. This energy is equal to the difference between the total incident energy I_0E_0 and the components of the energy absorbed in the oxide layer ($I_0\gamma_d\bar{E}_{ad}$), the energy backscattered in this layer ($I_0\eta_d\bar{E}_{bd}$), and the energy backscattered from the silicon crystal ($I_0\eta_{\mathrm{Si}}\bar{E}_{\mathrm{Si}}$):

$$\begin{aligned} I_A(\mathrm{Si})E_A(\mathrm{Si}) &= \{I_0E_0 - [I_0\eta_d\bar{E}_{bd} + I_0\gamma_d\bar{E}_{ad}]\} - \{I_0E_0 - [I_0\eta_d\bar{E}_{bd} + I_0\gamma_d\bar{E}_{ad}]\}(\eta_{\mathrm{Si}}\bar{E}_{\mathrm{Si}}/\bar{E}_T) \\ &= \{I_0E_0 - [I_0\eta_d\bar{E}_{bd} + I_0\gamma_d\bar{E}_{ad}]\}(1 - \eta_{\mathrm{Si}}\bar{E}_{\mathrm{Si}}/\bar{E}_T). \end{aligned} \quad (6)$$

Here, η_d and γ_d are, respectively, the electron backscattering and absorption coefficients in the protective film; $\bar{E}_{bd}$ and $\bar{E}_{ad}$ are, respectively, the energies of backscattered and absorbed electrons; and $\bar{E}_T$ is the energy of the electrons transmitted through the film. The expression in square brackets describes as a result the total energy loss in the film for the electrons excluded from generation of electron–hole pairs in a Si crystal. The electrons backscattered from the Si crystal are also excluded from this process; this exclusion is described by the factor $(1 - \eta_{\mathrm{Si}}\bar{E}_{\mathrm{Si}}/\bar{E}_T)$ in (6). Assuming that $\eta_{\mathrm{Si}} = 0.19$ [5] and estimating the average energy $\bar{E}_{\mathrm{Si}}$ from the simple empirical relation

$$\bar{E}/E = 1.08(1 - Z^{-0.3}), \quad (7)$$

where Z is the atomic number of the target material and E is the incident electron energy, we have $1 - \eta_{\mathrm{Si}}\bar{E}_{\mathrm{Si}}/\bar{E}_T = 0.886$.

In turn, the expression in braces in (6) is the total energy of the electron beam transmitted through the protective film, $I_T\bar{E}_T$. Formula (6) can now be written as

$$I_A(\mathrm{Si})E_A(\mathrm{Si}) = I_T\bar{E}_T \times 0.886. \quad (8)$$

According to [8], the electron current through a SiO_2 layer of thickness d is

$$I_T = I_0(1 - \eta_d)\exp\left[-4.6\left(\frac{d}{R(\mathrm{SiO_2})}\right)^2\right], \quad (9)$$

where the electron backscattering coefficient η_d for the protective oxide film can be determined in the first-order approximation from relation η_d =

$\eta_0(SiO_2)\left(1-\exp\left[\frac{-4d}{R(SiO_2)}\right]\right)$ [9]. The total range of incident electrons in the oxide can be calculated from the formula [10]

$$R\ [\text{нм}] = \frac{27.6AE_0^{1.67}\ [\text{keV}]}{\rho Z^{0.89}}, \quad (10)$$

where A is the atomic weight, Z is the atomic number, and ρ [g cm^{-3}] is the specific target density. In the case under consideration (for SiO_2 oxide), we have $\bar{Z} = 15.3$, $\bar{A} = 31$, and $\rho = 2.65$ g cm^{-3}; therefore, $R = 28.5\ E_0^{1.67}$. The electron backscattering coefficient for the SiO_2 bulk material is $\eta(SiO_2) = 0.2$; hence, expression (9) takes the form

$$I_T = I_0\left[0.8 + 0.2\exp\left(-\frac{4d}{R}\right)\right]\exp\left[-4.6\left(\frac{d}{R}\right)^2\right]. \quad (11)$$

The average energy E_T of the electrons transmitted through a layer of thickness d is determined by the relation [10]

$$\bar{E}_T = \left(1-\frac{d}{R}\right)^{0.6}E_0. \quad (12)$$

As a result, expression (8) is transformed as

$$I_A(\text{Si})E_A(\text{Si}) = 0.886I_0\left[0.8 + 0.2\exp\left(-\frac{4d}{R}\right)\right] \times \exp\left(-4.6\left(\frac{d}{R}\right)^2\right)\left(1-\frac{d}{R}\right)^{0.6}E_0. \quad (13)$$

When a detector is irradiated by a monoenergetic electron beam, the response signal, according to expression (2), is (at $E_i = 3.65$ eV and $CD = 0.646$)

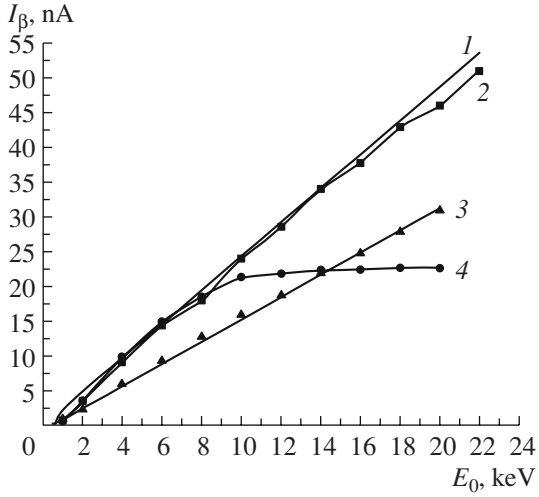

Fig. 1. Characteristics of the detector response signal under irradiation by a monoenergetic electron beam.

$$I_\beta = 0.157I_0E_0\left[0.8 + 0.2\exp\left(-\frac{4d}{R}\right)\right] \times \exp\left(-4.6\left(\frac{d}{R}\right)^2\right)\left(1-\frac{d}{R}\right)^{0.6}. \quad (14)$$

As a main backscattered electron detector, we used a silicon planar diode with a shallow p–n junction. The crystal surface area is 3×10 mm^2 and the n-type substrate resistivity is $1.5 \times 10^3\ \Omega$ cm; i.e., the dopant (phosphorus) concentration is 5×10^{12} cm^{-3}. The top 25-nm-thick p^+ layer has a high impurity (boron) concentration (10^{21}–10^{22} cm^{-3}). The width of the space-charge region is 10 μm; the carrier drift time in this region is approximately 10^{-8}–10^{-9} s; these values are several orders of magnitude smaller than the lifetime of nonequilibrium carriers in the neutral region of the n-type substrate, where the carrier diffusion length is about 100 μm. The barrier capacitance of the p–n junction is 230 pF and the dark current is 5×10^{-11} A (at a reverse bias of 10 mV). The top crystal surface was protected by a SiO_2 passivating layer. According to the experimentally determined threshold energy of the detector sensitivity, $E_{th} = 0.75$ keV, the estimation for d is 17 nm.

Figure 1 shows the calculated (curve *1*) and experimental (curve *2*) dependences of the response signal on the incident electron energy E_0 for the detector used by us (SPD-8UVHS [11, 12]). The experiments were performed on a scanning electron microscope with irradiation of a scanning platform 0.1×0.1 mm^2 in size by the probe current $I_0 = 0.01$ nA. Characteristics *1* and *2* differ only by the quality factor: $CD = 1$ and 0.89 for ideal and real diodes, respectively. The points of intersection of the curves with the E_0 axis give the threshold energies E_{th}. In the case studied here, $E_{th} = 0.6$ and 0.75 keV for the experimental and theoretical dependences, respectively. The experimental values of E_{th} are somewhat underestimated due to the accepted linear extrapolation of the curves at low primary electron energies ($E_0 < 1.5$ keV), which is not quite correct.

Let us now estimate the response function of the detector under consideration. For example, at the energy $E_0 = 10$ keV, the measured and calculated signals I_β are 24 and 24.38 nA, respectively. Hence, the quality factor $CD = 0.984$ and the experimental response function is $\Theta_{meas} = I_\beta/(I_0E_0/q) = 0.24$ A W^{-1}, whereas the theoretical value $\Theta_T = I_0(E_0/E_i)/I_0E_0 = 0.274$ A W^{-1}. The ratio of these functions is $\Theta_{meas}/\Theta_T = 0.876$, a value close to that of the most effective known semiconductor detectors: $\Theta_{meas}/\Theta_T = 0.888$ [4].

Curve *3* demonstrates deterioration of the I_β] characteristic of the same crystals due to the low value of D; in this case, since ohmic contacts are imperfect and leakage currents are present in the detection circuit, CD is only 0.646.

The crystal with a characteristic presented by curve *4* differs from the previous ones by nonlinearity and low efficiency. These drawbacks are due to the fact that the base of the *p–n* junction in this crystal has a lower resistivity, i.e., a narrow space charge region ($w < R_0$) and small diffusion length L. All these circumstances affect the quality factor, significantly deteriorating the general detector characteristic.

2. CHARACTERISTICS OF DETECTORS IRRADIATED BY A NONMONOENERGETIC ELECTRON BEAM

The above-considered pattern is significantly complicated when the entire spectrum of backscattered electrons is detected rather than a monoenergetic electron beam (for example, in SEMs). In this case, one has to consider the integral and differential characteristics of the electron beam, i.e., take into account both the number of detected electrons and their different fractal energy. Correspondingly, the quantities I_0, E_0, and $R(E_0)$ in expression (14) must be replaced. Instead of electrons with the same energy E_0, backscattered electrons with an average energy $\bar{E}$, estimated from relation (7), are incident on the detector, and the average primary electron range (in our case, in oxide) is taken to be

$$\bar{R} = \frac{1}{\eta(SiO_2)}\int_0^R \frac{\partial N}{\partial x}\, x dx.$$

Let us assume in the first-order approximation that $\bar{R}$ coincides with the total diffusion length x_0 of primary electrons, which is given by the expression [10]

$$x_0 = \bar{R} = [1/(1 + 0.187Z^{0.67})]R. \qquad (15)$$

For SiO_2, $\bar{Z} = 15.3$; therefore, $\bar{R} = 0.462\,R$ or, taking into account (10), R [nm] $= 0.462 \times 28.5\bar{E}^{1.67}$ [keV] $= 13.17\bar{E}^{1.67}$ [keV]. We also take into account that only some part of backscattered electrons are incident on the detector; this part is determined by the finite solid angle of electron collection $d\Omega$ and the electron backscattering coefficient η of the material studied; thus, the current component of the detected signal is $I_0\eta d\Omega$. With allowance for all these corrections, the main expression for the detected signal can be written as

$$I_\beta = 0.157 I_0 d\Omega \eta \bar{E}\left[0.8 + 0.2\exp\left(-\frac{4d}{R}\right)\right] \times \exp\left(-4.6\left(\frac{d}{R}\right)^2\right)\left(1 - \frac{d}{\bar{R}}\right)^{0.6}. \qquad (16)$$

The dependences $I_\beta(E_0)$ calculated from this formula for three reference bulk gold ($\eta_{Au} = 0.5$), copper ($\eta_{Cu} = 0.32$), and silicon ($\eta_{Si} = 0.19$) targets are shown in Fig. 2 (for clearness, the initial portions are shown enlarged in the inset). In the calculations, we assumed that $I_0 = 10$ nA and $d\Omega = 0.65 \times 10^{-3}$ sr and $\bar{R}$ and $\bar{E}$ were taken from relations (15) and (7), respectively; i.e., $\bar{E}(Au) = 0.79E_0$, $\bar{E}(Cu) = 0.69E_0$, and $\bar{E}(Si) = 0.59E_0$. The measurement results for the same samples are shown in Fig. 3. To measure the backscattered electron current $I_0 d\Omega\eta$, a Faraday cup with the same solid angle of electron collection $d\Omega$ was located near the semiconductor detector.

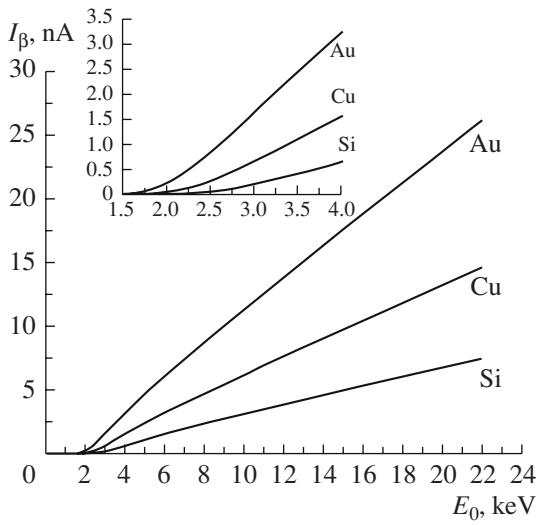

Fig. 2. Theoretical dependences of the detector response signal under irradiation by an electron beam with a wide energy spectrum.

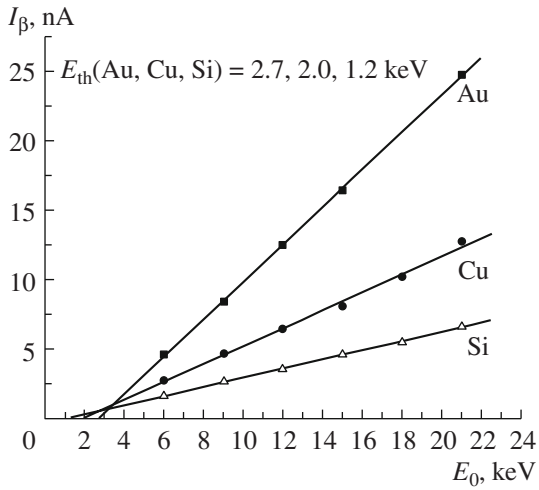

Fig. 3. Experimental dependences of the detector response signal under irradiation by an electron beam with a wide energy spectrum.

Comparison of the plots in Figs. 1–3 reveals a significant difference in the found values of the threshold energy E_{th} at which the signal $I_\beta = 0$; note that E_{th} is different not only for the cases of irradiation by a monoenergetic beam or wide-spectrum electron beams in

detection of backscattered electrons but also for targets of materials with different atomic numbers.

For example, for irradiation by a monoenergetic electron beam, $E_{th} \approx 0.75$ keV (Fig. 1), whereas, for detection of backscattered electrons from Au, Cu, and Si targets, the experimental values of E_{th} are, respectively, 2.7, 2, and 1.2 keV. The experimental energies E_{th} were determined from the points of intersection of the extrapolated plots $I_\beta = f(E_0)$ with the abscissa axis. We had to use extrapolation because at small values of E_0, close to E_{th}, the I_β signal is low (close to the noise level); therefore, exact measurements cannot be performed. The threshold energy E_{th} can be approximately estimated as follows. At two I_β signals, measured at two electron energies E_{01} and E_{02}, the equality [2] $\frac{I_{\beta 1}}{I_{\beta 2}} = \frac{E_{01} - E_{th}}{E_{02} - E_{th}}$ remains valid. This equality yields the energy E_{th}, whose experimental values for different targets are given in Fig. 3.

The calculated values of E_{th} can be estimated from the energy factor in expression (16). $I_\beta = 0$ at $\left(1 - \frac{d}{\bar{R}}\right)^{0.6} = 0$, i.e., at $d = \bar{R} = 13.17\bar{E}_{th}^{1.67}$. Taking into account that $d =$ 17 nm and $\bar{E}_{th} = cE_{0th}$, where $c = 0.79$, 0.69, and 0.59 for Au, Cu, and Si, respectively, we obtain $E_{0th} = 1.5$, 1.69, and 1.98 keV for the Au, Cu, and Si targets; these values coincide with the data in the inset in Fig. 2.

Comparison of Figs. 2 and 3 reveals a significant difference in the behavior of the experimental and calculated characteristics I_β in the region of their intersection with the energy axis E_0. This contradiction can be explained as follows. Deriving formula (16) and plotting the corresponding curves in Fig. 2, we assumed that the average backscattered electron energy $\bar{E}/E_0$ is a constant depending only on the atomic number Z of the target material. Since $\bar{E}/E_0$ (for example, for the Au target) is larger than that for the Si target, the detector response signal I_β is higher in the former case. Simultaneously, E_{th} in the I_β characteristic of the Au target decreases in comparison with that for the Si target.

However, the threshold value of the I_β cutoff signal depends not specifically on the average energy $\bar{E}$ of backscattered electrons but on the shape of their energy spectra (in other words, on the product of the number of backscattered electrons in a certain energy range by their energy in this range). It is specifically the magnitude of this product in the initial energy range (from zero to $E = E_{th}$) that determines the minimum value $I_{\beta min} =$ const for this detector:

$$I_{\beta min} = I_{ad}E_{th}/\bar{E} = \left[\frac{1}{N_0(Z)}\int_0^{E_{th}}\frac{\partial N}{\partial E}dE\right] \times \left[\frac{1}{R}\int_0^d \frac{\partial E}{\partial S}dS\right] = \text{const}. \quad (17)$$

This relation between the current and energy components of the threshold signal depends on the shape of the backscattered electron spectrum. In particular, for the Si target in the initial energy range (for example, from 0 to $0.5E_0$), the total number of backscattered electrons exceeds that for the Au target; therefore, the equality is satisfied if $E_{th}(\text{Si}) < E_{th}(\text{Au})$; this conclusion is confirmed by the experimental characteristics in Fig. 3. The second factor of the actual increase in E_{th} for the detection of signal from elements with a larger Z is as follows: higher energy electrons from each part of the backscattering spectrum are backscattered to a larger extent from the thin surface layer of the protective coating. However, the specific contribution of such electrons to the Au target spectrum exceeds that to the spectrum of the Si target; therefore, their separation at the oxide layer more significantly affects the $I_{\beta min}$ signal in the former case.

In any case, the discrepancy between the theoretical and experimental data on the threshold energy of semiconductor detectors of backscattered electrons requires further, more detailed, analysis.

CONCLUSIONS

The calculated and experimental characteristics of the response function of semiconductor detectors show their strong dependence on the following main factors: the presence of leakage currents in the detector circuit, the depth of the p–n junction, the width of the space charge region near the junction barrier, and the thickness and electron transparency of the protective passivating coating. The latter characteristic decisively determines the threshold energy E_{th} of detected electrons. This value, as was shown above, is significantly different for the cases of detection of monoenergetic electrons or the total energy spectrum of backscattered electrons.

The minimum detected signal in a semiconductor detector is a complex function depending on the shape of the energy spectrum (i.e., on the atomic number Z of the target material) and on the electron backscattering coefficient of the target under study. All these factors are of great practical importance both in production of detectors and in their application in experimental setups, in particular, SEMs.

ACKNOWLEDGMENTS

This study was supported in part by the Russian Foundation for Basic Research, project no. 06-08-01230-a.

REFERENCES

1. Gedcke, D.A., Ayers, J.B., and Denee, P.B., *Scanning Electron Microscopy*, O'Hare, Ed., Chicago, 1978, vol. 1, p. 581.
2. Lin, P.S. and Becker, R.P., *Scanning Electron Microscopy*, O'Hare, Ed., Chicago, 1975, p. 61.
3. Radzimski, Z.J., *Scanning Electron Microscopy*, O'Hare, Ed., Chicago, 1987, vol. 1, p. 975.
4. Funsten, H.O., Sunszcynsky, D.M., Ritzau, S.M., and Korde, R., *IEEE Trans. Nucl. Sci.*, 1997, vol. 44, no. 6, p. 2561.
5. Reimer, L., *Image Formation in Low-Voltage Scanning Electron Microscopy*, Washington: SPIE Press, 1993, p. 33.
6. Leamy, H.J., *J. Appl. Phys.*, 1982, vol. 53, no. 6, p. R51.
7. Sze, S.M., *Physics of Semiconductor Devices*, New York: Wiley, 1969. Translated under the title *Fizika poluprovodnikovykh priborov,* Moscow: Mir, 1984.
8. Fitting, H.J., *Phys. Status Solidi (a)*, 1974, vol. 26, p. 525.
9. Seiler, H., *J. Appl. Phys.,* 1983, vol. 54, p. R1.
10. Kanaya, K. and Okayama, S., *J. Phys. D: Appl. Phys.*, 1982, vol. 5, p. 43.
11. Scholze, F., Klein, R., and Muller, R., *Metrologia*, 2006, vol. 43, p. 6.
12. Alekseev, A.G., Belov, A.M., Zabrodsky, V.V., et al., *Plasma Fusion Res.*, 2007, vol. 2, p. 1061.